CELL CYCLE
2020, VOL. 19, NO. 19, 2496–2508
https://doi.org/10.1080/15384101.2020.1807670

Taylor & Francis
Taylor & Francis Group

RESEARCH PAPER

Elevated microRNA-7 inhibits proliferation and tumor angiogenesis and promotes apoptosis of gastric cancer cells via repression of Raf-1

Jing Lin[a], Zewa Liu[a], Shasha Liao[b], E Li[b], Xiaohua Wu[b], and Wanting Zeng[c]

[a]Oncology Department, The First Affiliated Hospital of Shantou University Medical College, Shantou, China; [b]Oncology Department, Shantou Longhu People's Hospital, Shantou, Guangdong, China; [c]MSci Applied Medical Science, Division of Medicine, University College London, London, WC1E 6BT, United Kingdom

ABSTRACT

Objective: Since the essential involvement of microRNAs (miRNAs) in the development and progression of GC, the study was for the exploration of the value of microRNA-7 (miR-7) in the evaluation of neoadjuvant chemotherapy for gastric cancer (GC) and its effects on apoptosis, proliferation and angiogenesis of GC.

Methods: miR-7 expression in serum of GC patients before and after neoadjuvant chemotherapy were detected to explore its role in neoadjuvant chemotherapy of GC. The GC cells were transfected with miR-7 mimics/inhibitors, or siRNA-Raf-1 to figure out their roles in proliferation, migration, invasion, cycle distribution and apoptosis. Tumor xenograft was conducted to test tumor growth. Microvessel density (MVD) in tumors was tested by immunohistochemical staining.

Results: miR-7 expression in serum of GC patients was lower than that of healthy controls while it was elevated after neoadjuvant chemotherapy. Moreover, higher miR-7 expression was exhibited in chemotherapy-effective patients rather than chemotherapy-ineffective patients ($P < 0.01$). miR-7 expression in serum was connected with tumor size, degree of differentiation, TNM stage and lymphatic metastasis.miR-7 was decreased and Raf-1 was elevated in GC cells (both $P < 0.05$). Elevated miR-7 or declined Raf-1 inhibited GC cell migration, proliferation and invasion, cell cycle entry, xenografted tumor growth and MVD and stimulated apoptosis (all $P < 0.05$). Down-regulated Raf-1 reversed the impacts of miR-7 knockdown on GC cells (all $P < 0.05$).

Conclusion: Our study highlights that elevated miR-27a indicates the good efficacy of neoadjuvant chemotherapy in GC and miR-7 targets Raf-1 to suppress tumor development and angiogenesis of GC cells.

ARTICLE HISTORY
Received 4 January 2020
Revised 1 July 2020
Accepted 1 August 2020

KEYWORDS
MicroRNA-7; gastric cancer; neoadjuvant chemotherapy; Raf-1; proliferation; migration; invasion; apoptosis

Introduction

Gastric cancer (GC) ranks the fourth common cancer and the second main reason for cancer-linked mortality [1]. There are many risk elements for GC, such as alcohol consumption, infection with helicobacter pylori, and organ damage from drug [2]. There are a plenty of treatment methods in clinical diagnostics, surgical techniques, and new chemotherapy regimens for GC [3]. Chemotherapy is still the main way to treat GC in clinics, while it also induces serious side effects to the patients due to the absence of selectivity [4]. Because of the unexpected survival, new therapeutic targets need exploring to attenuate prognosis of GC.

MicroRNA-7 (miR-7), the first intron of the heterogeneous ribonucleic acid protein K gene residing on chromosome 9, is highly conserved in all species and in functions, with its transmission stability in the different regulation system [5,6]. Studies have shown that miR-7 is not only involved in neuroendocrine tumors development such as malignant schwannoma [7], but also in human GC [8] and lung cancer [9] with its low expression. Abnormal expression level of miR-7 is related to many tumors and participates in the process of tumor development. Concerning to that, we hope to further study the mechanism of miR-7 involved in GC proliferation, apoptosis and angiogenesis. Although studies have reported that miR-7 expression is supposed to be a latent therapeutic approach for GC [10–13], miR-7 may function via different regulatory mechanisms and targets in GC. Given that, this work focuses on the effects of miR-7 targeting Raf-1 on GC proliferation, apoptosis and angiogenesis. As previously

CONTACT Jing Lin LLLinjing2019@163.com

reported, strengthened expression of miR-7 apparently decreased expression of Raf-1 and other elements [14]. That down-regulated miR-7 facilitates the activation of Raf-1 pathway and the induction of interleukin-6 (IL-6) [15]. Raf-1 is a serine threonine kinase that phosphorylates and makes a family of protein kinases termed MAP kinase or Mek alive [16]. As a primary member of Raf family, Raf-1 has been related to tumorigenesis, cell-cycle control and apoptosis, invasion and metastasis [17]. Raf-1 is possible to occupy a significant role in the angiogenesis of human GC and therapeutic methods targeting Raf-1 and Raf-1-mediated pathway may be a new avenue in GC intervention [17]. The study was started for the investigation of the value of miR-7 in the evaluation of neoadjuvant chemotherapy for GC and its effects on proliferation, apoptosis and angiogenesis of GC.

Materials and methods

Ethics statement

The study was permitted by the clinical trial Institutional Review Board of The First Affiliate Hospital, School of Medicine, Shantou University and followed the principles of *the Declaration of Helsinki*. All patients in this experiment signed informed consent. The protocol was allowed by the Institutional Animal Care and Use Committee of The First Affiliate Hospital, School of Medicine, Shantou University.

Collection of clinical data

From June 2015 to June 2016, 53 patients (28 males and 25 females) with GC who underwent neoadjuvant chemotherapy were collected. The patients were 38–75 years old with an average age of 57 years. Degree of differentiation: 37 cases of poor and moderate differentiation and 16 cases of high differentiation. Tumor node metastasis (TNM) staging: 34 patients in IIIb stage and 19 in stage IV. All patients were included if they met the following criteria: They were diagnosed by gastroscopy or cytology before surgery; GC patients were staged in advanced IIIb stage and IV stage with reference to TNM staging at the seventh edition of International Union Against Cancer/American Joint Committee on Cancer in 2010; None of patients had received radiotherapy, chemotherapy or other adjuvant therapy before admission; none of the patients was accompanied by contraindications to chemotherapy; Patients had measurable lesions according to Response Evaluation Criteria in Solid Tumors (RECIST1.1) [18]. Patients with distant metastases, other malignant tumors, severe heart disease or arrhythmia, or with a history of myocardial infarction within one year, or pregnant or lactating women were excluded. Another 53 healthy controls were selected from the medical examination center of The First Affiliate Hospital, School of Medicine, Shantou University.

GC patients were taken 10 mL of blood on an empty stomach in the morning before neoadjuvant chemotherapy. The blood was sent to the laboratory in 1 hour and the serum was extracted with 2.5 mL by the centrifuge, stored in cryotubes and put in a refrigerator at −80°C. After the neoadjuvant chemotherapy treatment (three cycles), the same method was used for collecting blood samples. The blood samples of 10 mL were obtained from healthy controls, centrifuged and stored at −80°C.

Neoadjuvant chemotherapy and efficacy assessment

Patients were intravenously injected with 5% glucose solution containing oxaliplatin (130 mg/m^2) on the first day and orally administrated with capecitabine (1000 mg/m^2) from the 1st day to the 14th day (21 days/cycle, for total 3 cycles). Neoadjuvant chemotherapy was assessed and re-operated after treatment. Antiemetic drugs were applied in treatment with oxaliplatin while oral liver protection, Baiyao and neurotrophic drugs in oral administration with capecitabine. The adverse reactions during chemotherapy were leukopenia (15 cases), nausea and vomiting (8 cases), abnormal liver function (7 cases), and diarrhea (3 cases). Abdominal CT or magnetic resonance

imaging of the patients before and after chemotherapy was compared, and the efficacy assessment was performed according to the RECIST 1.1. Efficacy evaluation was classified into four grades including complete response (CR, all tumor lesions disappeared, lasting for 4 weeks), partial response (PR, the sum of the longest diameter of the tumor was reduced by more than 30%, lasting for 4 weeks), stable disease (SD, ranked between PR and PD), and progressive disease (PD, the sum of the longest diameter of the tumor was increased by 20% with the appearance of new lesions). The chemotherapy efficacy was calculated as (CR + PR)/total cases × 100% [19].

Reverse transcription quantitative polymerase chain reaction (RT-qPCR)

Total RNA in serum samples and cells was extracted by Trizol (Invitrogen, Carlsbad, CA, USA). The quality of RNA was assessed by ultraviolet and formaldehyde denaturation electrophoresis. miR-7, Raf-1, U6 and β-actin primers were designed via using Primer premier 5.0 software with reference to the gene sequences in GenBank, and synthesized by Sangon Biotech Co., Ltd. (Shanghai, China) (Table 1). Then, the cDNA was extracted by using a reverse transcription kit (Beyotime Biotechnology Co., Ltd., Shanghai, China) referring to the instructions. The reaction solution was taken for fluorescence quantitative PCR. The relative expression of miR-7 was expressed with U6 as the internal reference, and the relative expression of Raf-1, β-actin. The relative expression of the target gene was calculated by the relative quantitative method $2^{-\Delta\Delta Ct}$.

Table 1. Primer sequences.

Gene	Primer sequences
miR-7	Forward: 5′-GGAAAGGCTCATTCGGACTA-3′
	Reverse: 5′-ACGACGCCACCAATCACT-3′
U6	Forward: 5′-TCAGTTTGCTGTTCTGGGTG-3′
	Reverse: 5′-CGGTTGGCTGGAAAGGAG-3′
Raf-1	Forward: 5′-GCAGGATAACAACCCATTC-3′
	Reverse: 5′-GGTCAGCGTGCAAGCATT-3′
β-actin	Forward: 5′-GTGGGGCGCCCAGGCACCA-3′
	Reverse: 5′-CTCCTTAAGTCACGCACGTTTC-3′

Note: miR-7, microRNA-7

Cell culture

RGM-1 normal gastric mucosal epithelial cells, human GC cell BGC823 (Shanghai Institute of Biochemistry and Cell Biology, Chinese Academy of Sciences, Shanghai, China), human GC cell MGC-803 (Shanghai Institutes for Biological Sciences, Shanghai, China), and human GC cell SGC-7901 (Cell resource center, Chinese Academy of Sciences, Shanghai, China) were seeded in RPMI1640 medium with 100 ml/L fetal bovine serum (FBS) and 100 μg/mL penicillin, cultured with 5% CO_2 and saturated humidity at 37°C. After fully adherent to the wall, the cells were detached and sub-cultured in trypsin of concentration of 2.5 g/L. Cells in logarithmic growth phase were collected for subsequent experiments. The relative expression levels of the target genes in each group were determined by RT-qPCR. The two GC cell lines with largest or smallest differences of the relative expression of the target gene by contrast with RGM-1 cells were used for subsequent cell experiments.

Dual luciferase reporter gene assay

The target site for the binding relationship of Raf-1 and the corresponding miR-7 was predicted by online prediction software (http://www.microrna.org/microrna/home.do). The primers were designed and synthesized with the 3 untranslated region (UTR) sequence of Raf-1 gene. Forward and reverse primers were introduced into the restriction enzyme sites of restriction endonucleases Hind III and Spe I. The mutation sequence of the binding site was designed, and the target sequence fragment was synthesized by Genscript Biotechnology Co., Ltd. (Nanjing, China). The amplified target products and the pMIR-REPORT™ Luciferase vector plasmid were digested via restriction endonuclease Hind III and Spe I. The enzyme-digested product was recycled, ligated with T4 DNA ligase, and transformed with DH5α competent cells. The single colony was chosen and shaken, and the plasmid was extracted. The correct recombinant wild type (WT) and mutant

type (MUT) plasmids were received by enzyme digestion, sequencing and identification. In a 12-well plate, 1×10^5 BGC-823 and SGC-7901 cells were seeded into each well and co-transfected with the recombinant WT/MUT plasmids and miR-7 mimics/mimics NC for 48 h, and the cell culture fluid was discarded. Each well was added with 100 μL cell lysate in luciferase kit for lysing of 30 min. LAR II with 100 μL was joined to 20 μL cell lysate, and the fluorescence (A) was measured. The fluorescence value (B) was measured with the supplemented of 100 μL Stop&Glo reagent. The luciferase activity value C = B/A, with A as an internal reference.

Cell transfection

BGC-823 and SGC-7901 cells were transfected with negative control (NC) of miR-7 mimics, miR-7 mimics, NC of si-Raf-1, si-Raf-1, miR-7 inhibitor + si-Raf-1 NC, or miR-7 inhibitor + si-Raf-1. MiR-7 mimics, mimics NC and miR-7 inhibitors were purchased from Shanghai GenePharma Co., Ltd. (Shanghai, China). siRNA-Raf-1 and siRNA-Raf-1 NC were synthesized by Shanghai Sangon Biotechnology Co. Ltd. (Shanghai, China). When the cell confluence was 70%-80%, the MGC-823 and SGC-7901 cells were transiently transfected by lipofectamine2000 (Invitrogen, Carlsbad, California, USA). After transfection for 6 hours, the culture medium was changed and then cell lines were continually cultured for 48 h.

Cell proliferation assay

The cells in logarithmic phase transfected for 48 h were detached with 2.5 g/L trypsin. The cells (1×10^3 cells/100 μL/well) were cultured in a humidified incubator with 3 duplicate wells in each group. The CCK-8 method was used for detection at 24^{th} h, 48^{th} h and 72^{nd} h, respectively. CCK-8 solution (Dojindo Laboratories, Kumamoto, Japan) with 10 μL was joined to each well. After 4-h reaction under normal conditions, the optical density (OD, 450 nm) value of cells was measured by a microplate reader.

Cell migration and invasion detection

The cells at 48 h post transfection were trypsinized and re-suspended with RPMI-1640 medium to reach 1×10^5 cells/mL. The cell suspension (200 μL) was added to each well. RPMI-1640 medium with 500 μL was joined to the lower chamber of the Transwell chamber (Millipore, MA, USA). The culture medium in the upper chamber was removed. The cells were fixed with 95% ethanol and the chamber membrane was taken out. After fixation and staining, the membrane was observed under an inverted microscope. Five fields were chosen for counting the number of transmembrane cells. Three parallel reaction wells were set for each sample. Matrigel (Millipore) was thawed in a refrigerator at 4°C, and diluted with RPMI-1640 medium at a ratio of 1:8. The diluted solution with 100 μL was joined to the upper Transwell chamber, air-dried at 4°C, and coagulated overnight for later use. The remaining steps were the same as the Transwell migration experiment. Three parallel reaction wells were set for each sample.

Cell cycle and apoptosis detection

The transfected cells after 48 h were trypsinized, centrifuged, and added with pre-cooled ethanol with a concentration of 700 g/L ethanol and fixed at 4°C. After centrifugation, the cells were stained with propidium iodide (PI, BD Biosciences, CA, USA) in darkness, and the cell cycle was measured by a flow cytometer.

The transfected cells after 48 h were trypsinized and centrifuged. Cells with 1 mL were centrifuged and re-suspended by adding 200 μL of the binding buffer to attain 1×10^4 cells/mL. Annexin V with 5 μL and 5 μL of PI (both from BD Biosciences) were joined for staining. The binding buffer (400 μL) was added into cells for testing cell apoptosis rate on a flow cytometer.

Western blot analysis

Total protein of the cells was extracted by total cell protein extraction kit (Beyotime Biotechnology Co., Ltd., Shanghai, China). The concentration and purity

of the extracted total protein were detected by bicinchoninic acid method. A sample with 30 μg of the protein was applied into sodium dodecyl sulfate polyacrylamide gel electrophoresis (120 g/L). Then the protein was transferred and blocked. The membrane was joined with primary antibody Raf-1 (1:500), β-actin (1:500) and with the horseradish peroxidase-labeled secondary antibody (1:2000, all from Cell Signaling Technology, Beverly, MA, USA). The protein was exposed by chemical coloration, and analyzed by gel electrophoresis imager and the Quantity One software. Target protein expression was calculated with β-actin as the internal reference.

Tumor xenograft in nude mice

Forty-two BALB/c nude mice (4 ~ 5 weeks old) were purchased from Hunan SLAC Laboratory Animal Co., Ltd. (Changsha, China). The nude mice were raised under specific pathogen-free conditions, and acclimated to the new environment in the animal room for one week. The state of the animals was observed every day with disinfected food and water supply. The transfected GC BGC-823 cells and SGC-7901 cells were made for a single cell suspension. The PBS and Matrigel were mixed at 1: 1. The mixture was employed for cell re-suspension to 2×10^7 cells/mL. The nude mice were fixed and subcutaneously injected with the transfected cells in the back of hind legs under aseptic conditions. Each group of nude mice was inoculated with a kind of cell. The changes in mental status, diet and body weight of the nude mice were observed regularly. From the day of inoculation, the subcutaneous tumors of nude mice were observed every other day, and the length (L), width (W) and height (H) of the tumor nodules were measured every 3 days. The formula for calculating the tumor volume was: $V = \pi/6 (L \times W \times H)$. After 30 days, the nude mice were euthanized and the tumor was exfoliated. The specimen was fixed with 40 g/L formaldehyde, embedded in paraffin, and sectioned (about 4 μm).

Immunohistochemical staining

Paraffin section was dewaxed by conventional xylene, and dehydrated with gradient ethanol. Endogenous peroxidase activity was blocked via 30 mL H_2O_2. The sections were incubated with Histostain^{TM}-Plus reagent A (goat serum blocking solution, Beijing Zhongshang Golden Bridge Biotechnology Co., Ltd., Beijing, China). Then the sections were incubated with primary mouse CD34 monoclonal antibody (1:50, Cell Signaling Technology). The sections were incubated with Histostain^{TM}-Plus Reagent B (biotinylated secondary antibody, Beijing Zhongshang Golden Bridge Biotechnology Co., Ltd., Beijing, China), and then Histostain^{TM}-Plus Reagent C (horseradish peroxidase-labeled third antibody, Beijing Zhongshang Golden Bridge Biotechnology Co., Ltd., Beijing, China). The sections were treated with diaminobenzidine color development, hematoxylin counterstaining, gradient ethanol dehydration, permeabilization with xylene, and sealing with neutral gum. After that, five randomly selected high-power fields were utilized to count the average proportion of positive cells in each field via the true color multifunctional cell image analysis management system (Image-Pro Plus, Media Cybernetics, USA). PBS was used instead of the primary antibody as an NC.

Statistical analysis

Statistical analysis was performed via using SPSS 21.0 statistical software (IBM Corp. Armonk, NY, USA). The measurement data were expressed as mean ± standard deviation. The measurement data following normal distribution between two groups were compared by independent sample t-test. One-way analysis of variance (ANOVA) was used for comparison of multiple groups. Tukey's multiple comparisons test was employed for pairwise comparison. The difference was considered statistically significant at $P < 0.05$.

Results

miR-7 expression is elevated in serum of patients with GC after neoadjuvant chemotherapy

A previous study has documented that miR-7 is downregulated in GC tissues versus to normal tissues [20]. Due to the down-regulated miR-7 in the tumor development, it is likely to be a potential target for tumor therapy. RT-qPCR was used to

detect miR-7 in serum of patients with GC before and after neoadjuvant chemotherapy (Figure 1a). It was manifested that miR-7 in GC patients before neoadjuvant chemotherapy was apparently lower in contrast with that in healthy controls ($P < 0.05$). miR-7 expression was distinctly rising after neoadjuvant chemotherapy of three cycles by contrast with that before neoadjuvant chemotherapy, hinting that miR-7 was connected with neoadjuvant chemotherapy in GC. Analysis of the relationship between miR-7 expression in serum before chemotherapy and clinicopathological data highlighted that miR-7 expression was correlated with tumor size, degree of differentiation, TNM stage and lymphatic metastasis (all $P < 0.05$, Table 2).

The efficacy of neoadjuvant chemotherapy in 53 patients was evaluated by RECIST 1.1. It turned out that there were two cases with CR, 26 cases with PR, 21 cases with SD and 4 cases with PD, with the efficacy rate at 52.83%, that was, 28 patients were in the effective group and 25 in the ineffective group. The expression of miR-7 in the serum of GC patients in the effective group was higher than that in the ineffective group ($P < 0.01$, Figure 1b). To analyze the predictive value of serum miR-7 in neoadjuvant chemotherapy sensitivity, receiver operating characteristic curve was utilized. The area under curve of miR-7 expression was 0.844, and the sensitivity and specificity were 85.7% and 76.0% (Figure 1c), indicating that miR-7 expression was predictive in neoadjuvant chemotherapy efficacy in GC.

Table 2. The correlation between miR-7 expression in serum of gastric cancer patients and clinicopathological features.

Clinicopathological features	Total (n = 53)	miR-7 expression in serum	*P*
Age (years)			
≥ 60	29	0.419 ± 0.167	0.670
< 60	24	0.400 ± 0.152	
Gender			
Male	28	0.408 ± 0.153	0.892
Female	25	0.414 ± 0.168	
Tumor size (cm)			
≥ 3	28	0.350 ± 0.145	0.003
< 3	25	0.478 ± 0.149	
Differentiation degree			
High	16	0.523 ± 0.157	<0.001
Moderate + poor	37	0.361 ± 0.135	
TNM staging			
IIIb stage	34	0.445 ± 0.140	0.032
IV stage	19	0.348 ± 0.176	
Lymphatic metastasis			
Yes	39	0.371 ± 0.149	0.002
No	14	0.519 ± 0.139	

miR-7 is down-regulated and Raf-1 is up-regulated in GC cells; Raf-1 is a target gene of miR-7

A study has revealed that miR-7 expression is reduced in GC cell lines and negatively connected with invasion and metastasis [21]. The relative expression of miR-7 in human normal gastric mucosal epithelial cell line RGM-1 and human GC cell lines (BGC-823, MGC-803 and SGC-7901) were tested by RT-qPCR, and highly expressed cell lines were screened. The results indicated that by contrast with RGM-1 cells, decreased miR-7 and raised Raf-1expression were manifested in GC cell lines (all $P < 0.05$) (Figure 2a–c). Among them, miR-7 had the highest

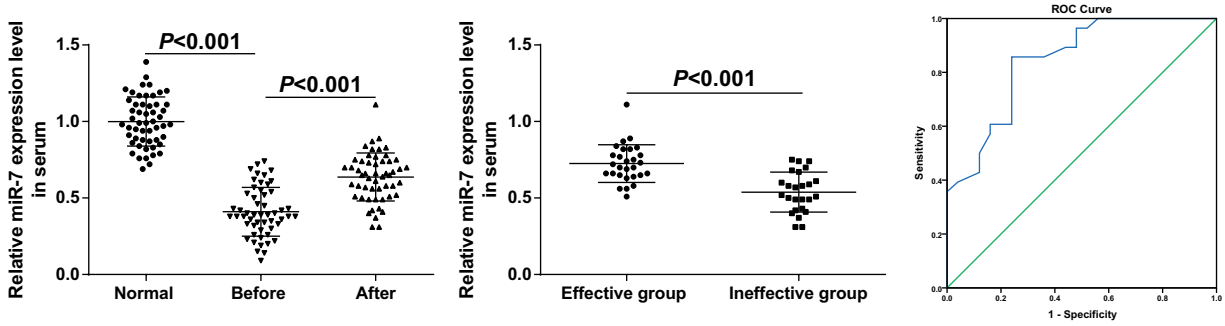

Figure 1. miR-7 is elevated in serum of patients with GC after neoadjuvant chemotherapy. (a). The relative expression of miR-7 in serum of 53 healthy controls and 53 patients with GC before and after neoadjuvant chemotherapy; (b). The relative expression of miR-7 in the serum of the effective group and the ineffective group after neoadjuvant chemotherapy; (c). Diagnostic efficacy of serum miR-7 expression in patients with GC after neoadjuvant chemotherapy by ROC curve analysis; In Figure (a)&(b), measurement data were mean ± standard deviation and compared by independent sample t-test.

relative expression in MGC-823 cells, and relatively low expression in SGC-7901 cells. Therefore, these two GC cells were selected for subsequent cell experiments and *in vivo* experiments in nude mice.

The http://www.microrna.org/microrna/home.do website predicted that Raf-1 contained two miR-7 target sequences (Figure 2d,f). To confirm that the predicted binding site of miR-7 caused a change in luciferase activity, the MUT sequence and WT sequence of Raf-1 3 -UTR were inserted into the reporter plasmid, respectively. Through dual luciferase activity assay, GC cells BGC-823 and SGC7901 were co-transfected with miR-7 mimics and WT-Raf-1 or MUT-Raf-1 recombinant plasmid, respectively. The results conveyed (Figure 2e,g), in BGC-823 cells, miR-7 mimics had no apparent effect on the luciferase activity of the MUT-Raf-1 plasmid ($P > 0.05$), but the luciferase activity of the WT-Raf-1 plasmid was distinctly reduced ($P < 0.05$). The same trend also existed in SGC-7901 cells.

For clarification of the role of miR-7 and Raf-1 in GC cells, miR-7 mimics/inhibitors and Raf-1 siRNA were transiently transfected into BCG-823 and SGC-7901 cells, respectively. It was determined that miR-7 up-regulation or Raf-1 down-regulation affected Raf-1 mRNA. Western blot analysis confirmed that miR-7 inhibited Raf-1 protein expression. Spontaneously down-regulating Raf-1 and miR-7 decreased Raf-1 expression versus to down-regulating miR-7 alone, indicating that Raf-1 down-regulation effectively mitigated the effects of miR-7 knockdown on Raf-1 expression in GC cells (Figure 2h–j)

GC cell proliferation is inhibited while apoptosis is promoted *in vitro* by elevated miR-7 and reduced Raf-1

For clarification of the functions of miR-7 and Raf-1 in GC cell proliferation and apoptosis, CCK-8 assay was utilized in testing OD values of cells at 24th h, 48th h, and 72nd h (Figure 3a,b) while PI single staining and Annexin V/PI double staining were in testing cell cycle entry and apoptosis rate (Figure 3c–g). The results showed that transfection of miR-7 mimics or Raf-1 siRNA could reduce GC cell proliferation, increased the proportion of G_1 phase cells, decreased the proportion of S phase and G_2/M phase cells and increased apoptosis rate. However, inhibition of miR-7 had the opposite effects. The effect of down-regulated miR-7 on GC cells could be reversed by Raf-1 knockdown, as manifested by impaired cell proliferation activity and enhanced apoptosis rate. These results indicated that miR-7 could target Raf-1 to affect cell proliferation and apoptosis of GC cells.

GC cell migration and invasion are repressed by increased miR-7 and decreased Raf-1

The effects of miR-7 and Raf-1 on GC cell migration and invasion were determined by Transwell assay (Figure 4a–d). It was recognizable that cell migration and invasion ability were weakened by miR-7 mimics or si-Raf-1 transfection. si-Raf-1 transfection reversed the promoting effects of miR-7 inhibitors treatment on cell migration and invasion ability. SGC7901 cells also had the same trend.

Tumor growth and angiogenesis are depressed by up-regulation of miR-7 and silencing of Raf-1

In addition, to verify the role of miR-7 and Raf-1 in the growth of xenografted tumors, BGC-823 and SGC-7901 cells transfected with miR-7 mimics/inhibitors or Raf-1 siRNA were injected into nude mice to observe tumor growth. Since tumors showing up on the 14th day, tumor volume was measured. The results demonstrated that miR-7 mimics or Raf-1 siRNA treatment reduced tumor volume and weight (Figure 5a–f).

At the same time, immunohistochemical staining of CD34 was utilized to quantitatively observe MVD. It could be recognized that CD34 could be detected in xenografted tumors after miR-7 up-regulation or Raf-1 down-regulation. Raf-1

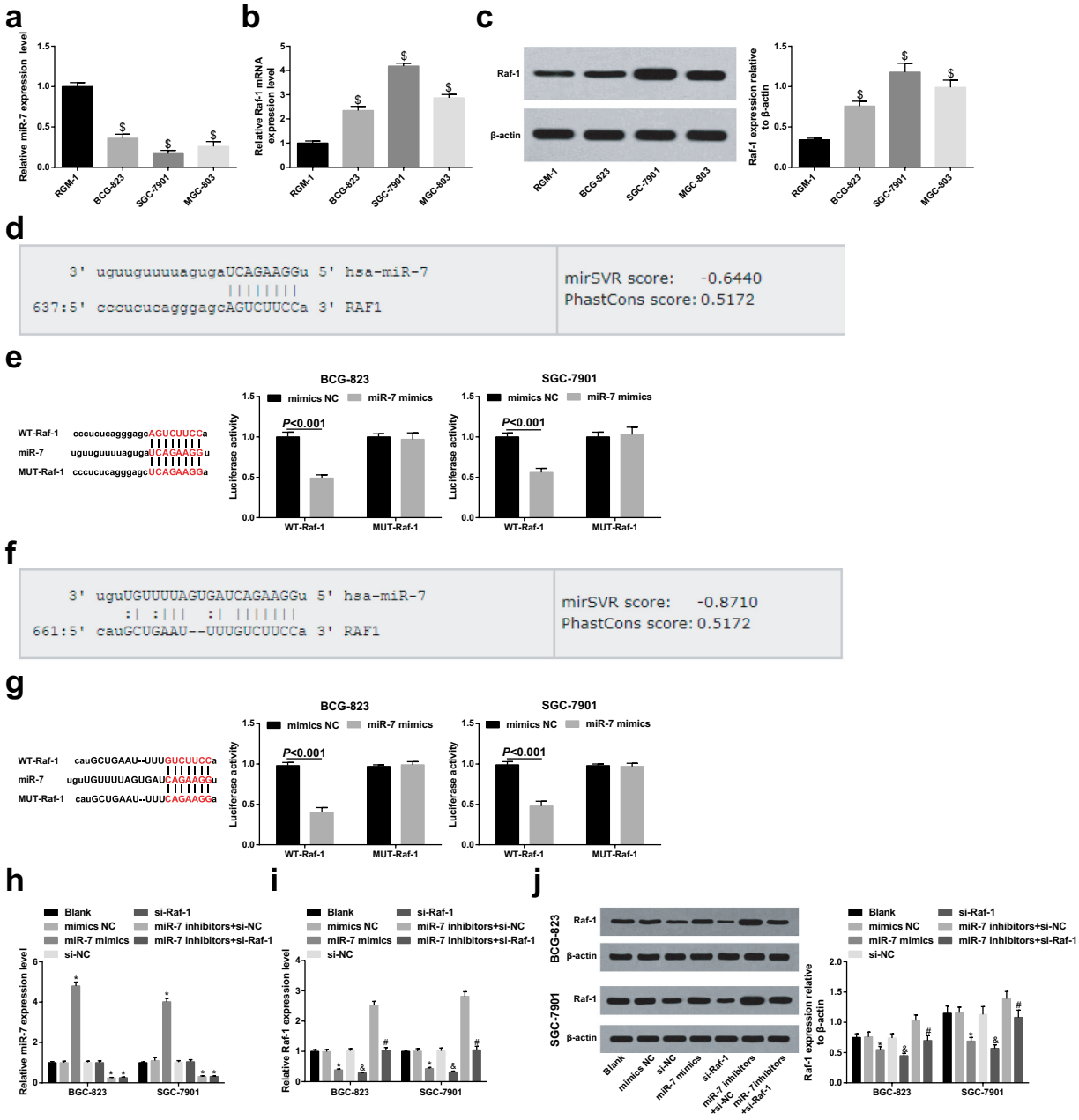

Figure 2. miR-7 is down-regulated and Raf-1 is up-regulated in GC cells; Raf-1 is a target gene of miR-7. (a). The relative expression of miR-7 in human normal gastric mucosal epithelial cell line RGM-1 and GC cell lines; (b). The relative expression of Raf-1 mRNA in human normal gastric mucosal epithelial cell line RGM-1 and GC cell lines; (c). Raf-1 protein bands and protein expression in human normal gastric mucosal epithelial cell line RGM-1 and GC cell lines; (d)&(f). The binding site of Raf-1 and miR-7 predicted by bioinformatics website; (e)&(g). The binding relationship between miR-7 and Raf-1 analyzed by dual luciferase reporter gene assay; (h). The relative expression of miR-7 after transfection in each group of cells; (i). The relative expression of Raf-1 mRNA after transfection in each group of cells; (j). The protein bands and protein expression of Raf-1 after transfection in each group of cells; $ vs the normal gastric mucosal epithelial cells RGM-1, $P < 0.05$; * vs the mimics NC group, $P < 0.05$; & vs the si-NC group, $P < 0.05$; # vs the miR-7 inhibitors + si-NC group, $P < 0.05$; Measurement data were mean ± standard deviation of three independent experiments. One-way ANOVA was utilized for data analysis among multiple groups, followed by Tukey's multiple comparisons test.

depletion followed by miR-7 inhibition reduced CD34 content in xenografted tumors. Raf-1 expression was noticed to positively connect with MVD, that was, increasing miR-7 or inhibiting Raf-1 could reduce angiogenesis and tumorigenesis of GC cells (Figure 5g,h).

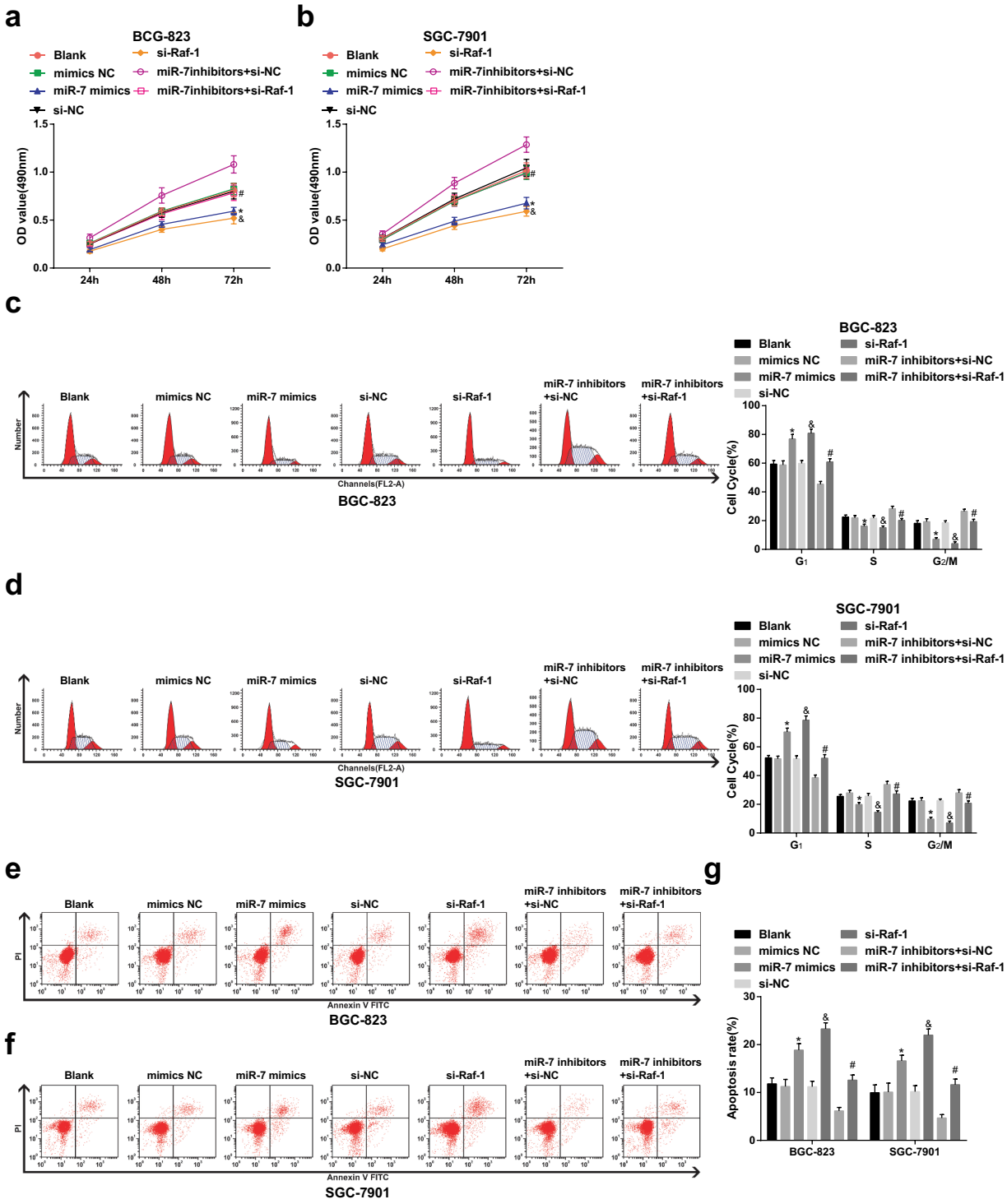

Figure 3. GC cell proliferation is depressed and apoptosis is promoted *in vitro* by elevated miR-7 and reduced Raf-1. (a)&(b). The change of BCG-823 and SGC-7901 cell proliferation ability after transfection; (c)&(d). The comparison of cell cycle distribution; (e–g). The comparison of cell apoptosis rate; * vs the mimics NC group, $P < 0.05$; & vs the si-NC group, $P < 0.05$; # vs the miR-7 inhibitors + si-NC group, $P < 0.05$; Measurement data were mean ± standard deviation of three independent experiments. One-way ANOVA was utilized for data analysis, followed by Tukey's multiple comparisons test.

Discussion

GC is a disease connected with a variety of elements including environmental factors [22]. A report has shown that knockdown of tumor suppressor miR-7 is one of the tumor-facilitating mechanisms based on the role of inflammation in

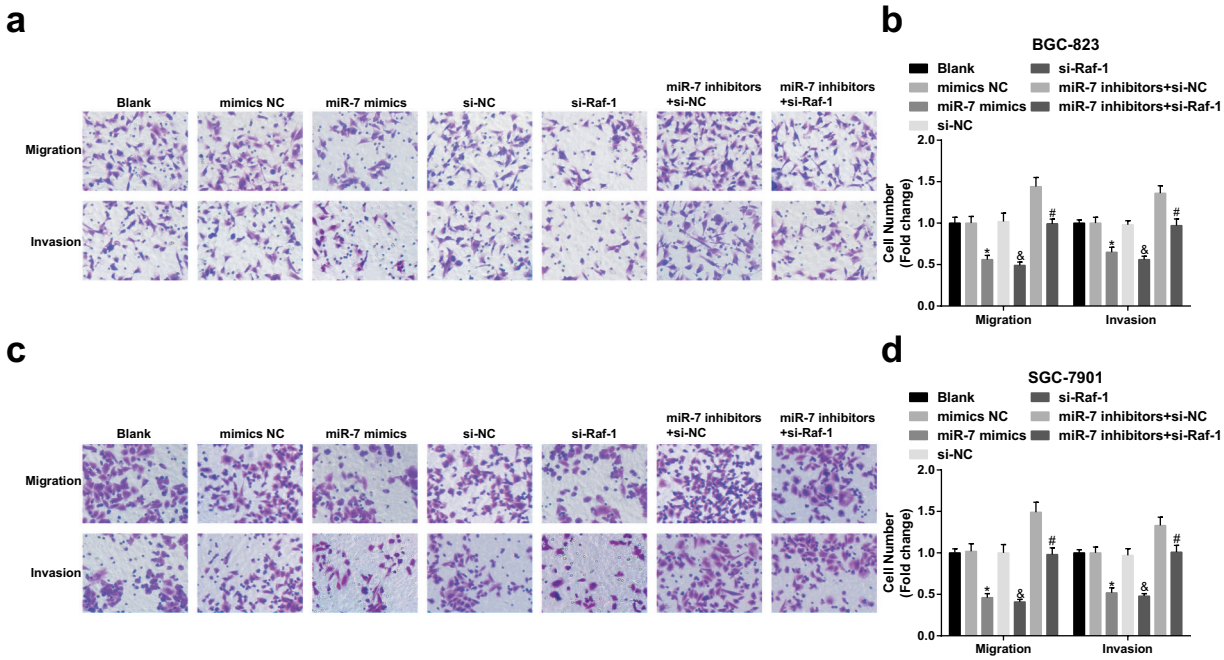

Figure 4. GC cell migration and invasion are repressed by up-regulated miR-7 and reduced Raf-1. (a)&(b). The number of migrating and invasive BGC-823 cells; (c)&(d). The number of migrating and invasive SGC-7901 cells; * vs the mimics NC group, $P < 0.05$; & vs the si-NC group, $P < 0.05$; # vs the miR-7 inhibitors + si-NC group, $P < 0.05$; Measurement data were mean ± standard deviation of three independent experiments. One-way ANOVA was utilized for data analysis, followed by Tukey's multiple comparisons test.

gastric tumorigenesis [23]. There is strong evidence that Raf-1 plays a significant role in the angiogenesis of human GC [24]. The study was for the investigation of the value of miR-7 in the evaluation of neoadjuvant chemotherapy for GC and its effects on proliferation, apoptosis and angiogenesis of GC cells. Collectively, the obtained results demonstrated that inhibited proliferation, migration, invasion, tumor angiogenesis and promoted apoptosis of GC cells were performed by upregulated miR-7 and downregulated Raf-1.

The major finding of this work showed that miR-7 was downregulated in GC and it was elevated in serum of patients with GC after neoadjuvant chemotherapy. A study has indicated that neoadjuvant chemotherapy has been functioned as a treatment approach for some solid tumors, such as breast, colorectal and advanced epithelial ovarian carcinoma [25]. There is another study suggesting that miR-145 and miR-185 expression increased apparently in GC patients after neoadjuvant chemotherapy [26], which is accorded with our results. Accordingly, miR-7 is restrained in GC cell lines, and its expression is connected with GC metastasis [21]. A same finding was that miR-7 is apparently repressed in GC tissues and cells [27]. Furthermore, we have confirmed the involvement of elevated Raf-1 in GC cells. A prior study that has noted the importance that Raf-1 is overexpressed in GC cell lines in contrast with GES-1 cells [24]. Elevated Raf-1 protein expression occurred as a regular event in human GC cells [17]. A strong relationship between miR-7 and Raf-1 has been reported in this study, which revealed that down-regulated Raf-1 expression was achieved by increased miR-7 after cell transfection. Consistently, there are also positive findings that the two target genes PI3K and Raf-1 were effectively decreased by the single-stranded rising miR-7 [14]. This is consonant with the fact that decreasing miR-7 is helpful to lapatinib-induced Raf-1 activation in regulating MAPK/AP-1 activation and IL-6 production [15].

In this work, we have presented evidence implicating that repressed GC cell migration, proliferation and invasion, tumor growth rate and volume, staining intensity and MVD and accelerated apoptosis showed up by elevated miR-7. As reported, GC cell lines transfected with miR-7 precursor apparently curbs cell proliferation, and overexpressed miR-7 in the GC cells represses tumor cell migration and invasion [28]. Similarly, another study has indicated repressed miR-7 in the tissue of GC and gastritis, and

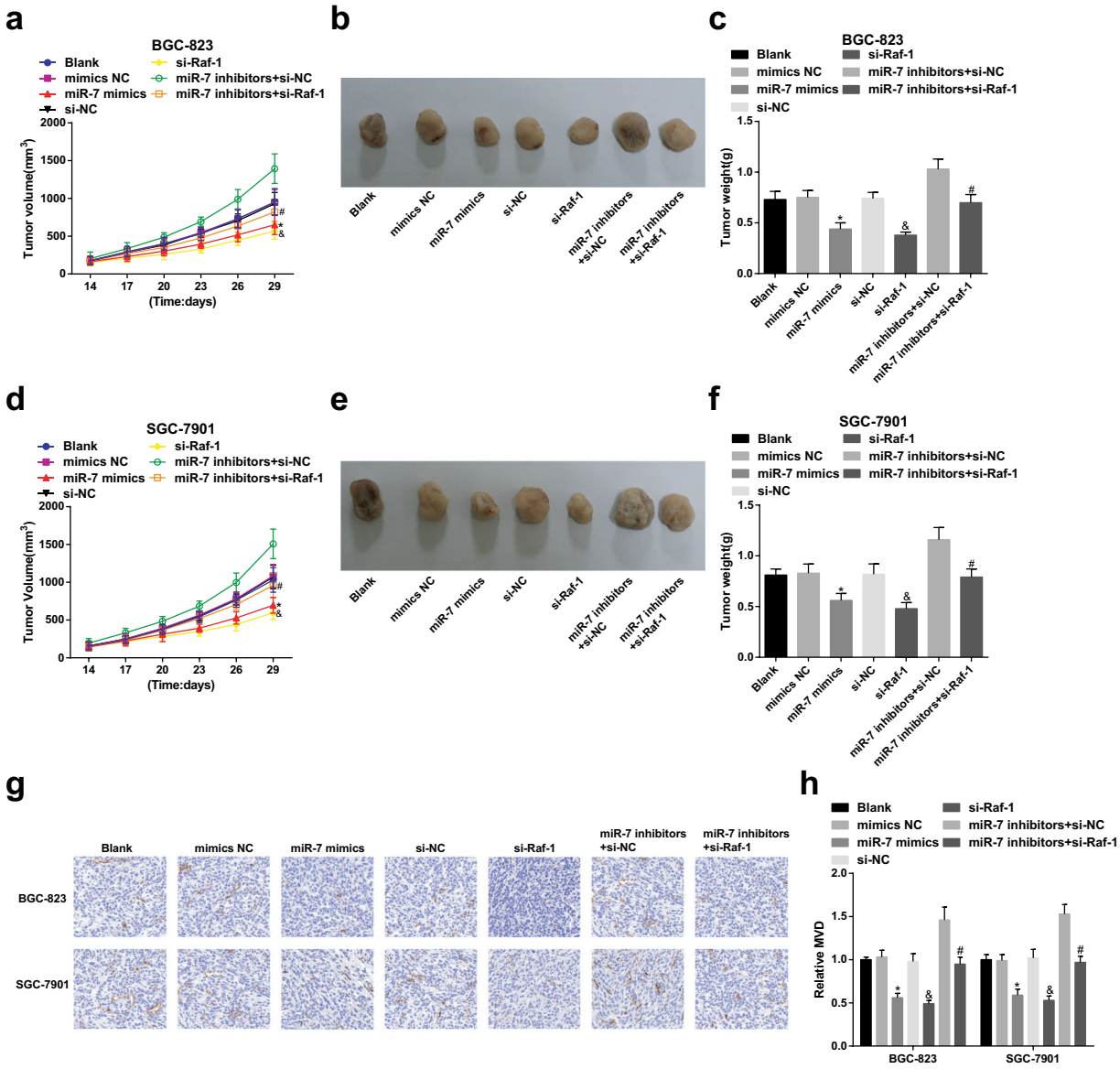

Figure 5. Tumor growth and angiogenesis are depressed by up-regulation of miR-7 and silencing of Raf-1. (a). Tumor growth curve of BGC-823 cells; (b). Representative tumors in mice injected with the transfected BGC-823 cells; (c). Tumor weight in mice injected with the transfected BGC-823 cells; (d). Tumor growth curve of SGC-7901 cells; (e). Representative tumors in mice injected with the transfected SGC-7901 cells; (f). Tumor weight in mice injected with the transfected SGC-7901 cells; G&H. CD34 expression and the number of new vessels in tumors; * vs the mimics NC group, $P < 0.05$; & vs the si-NC group, $P < 0.05$; # vs the miR-7 inhibitors + si-NC group, $P < 0.05$; Measurement data were mean ± standard deviation of three independent experiments. One-way ANOVA was utilized for data analysis, followed by Tukey's multiple comparisons test.

miR-7 restrains metastasis and invasion by aiming at epidermal growth element receptor or insulin-like growth factor-1 receptor [29]. Meanwhile, our research also suggested that repressed GC cell progression, tumor growth, staining intensity and MVD were presented by decreased Raf-1. This finding was also showed up by Meng *et al.* that knocking down Raf-1 strengthens GC cell apoptosis and inhibits cellular proliferation *in vitro* while inhibiting Raf-1 results in impairments in angiogenesis and tumor growth in GC [24]. This finding was also reported that decreased Raf-1 restrains the proliferation and facilitates the apoptosis of SGC7901 cells in GC [17].

In summary, our study conveys that upregulated miR-7 and downregulated Raf-1 suppress tumor development and angiogenesis in GC cells. This finding has important implications for exploring the pathogenesis of GC. The results of this paper can be further verified to identify additional targets and pathways of miR-7 in the future.

Acknowledgments

We would like to acknowledge the reviewers for their helpful comments on this paper.

Disclosure statement

The authors declare that they have no conflicts of interest.

Funding

This work was supported by Shantou Medical and Health Technology Project (No.180418184011332) (Jing Lin).

References

[1] Parisi A, Cortellini A, Roberto M, et al. Weight loss and body mass index in advanced gastric cancer patients treated with second-line ramucirumab: a real-life multicentre study. J Cancer Res Clin Oncol. 2019;145(9):2365–2373.

[2] Su T, Li F, Guan J, et al. Artemisinin and its derivatives prevent Helicobacter pylori-induced gastric carcinogenesis via inhibition of NF-kappaB signaling. Phytomedicine. 2019;63:152968.

[3] Quintero AG, Salgado M, Candamio S et al. First-line panitumumab plus docetaxel and cisplatin in advanced gastric and gastro-oesophageal junction adenocarcinoma: results of a phase II trial. Clin Transl Oncol. 2020;22:495–502.

[4] Zhang J, Zhao T, Han F, et al. Photothermal and gene therapy combined with immunotherapy to gastric cancer by the gold nanoshell-based system. J Nanobiotechnology. 2019;17(1):80.

[5] Feng R, Chen X, Yu Y, et al. miR-126 functions as a tumour suppressor in human gastric cancer. Cancer Lett. 2010;298(1):50–63.

[6] Kogo R, Mimori K, Tanaka F, et al. Clinical significance of miR-146a in gastric cancer cases. Clin Cancer Res. 2011;17(13):4277–4284.

[7] Saydam O, Senol O, Wurdinger T, et al. miRNA-7 attenuation in Schwannoma tumors stimulates growth by upregulating three oncogenic signaling pathways. Cancer Res. 2011;71(3):852–861.

[8] Asthana AK, Tandon SC, Pant GC, et al. Radiation therapy for symptomatic vertebral haemangioma. Clin Oncol (R Coll Radiol). 1990;2(3):159–162.

[9] Xiong S, Zheng Y, Jiang P, et al. MicroRNA-7 inhibits the growth of human non-small cell lung cancer A549 cells through targeting BCL-2. Int J Biol Sci. 2011;7(6):805–814.

[10] Li C, Li M, Xue Y. Downregulation of CircRNA CDR1as specifically triggered low-dose Diosbulbin-B induced gastric cancer cell death by regulating miR-7-5p/REGgamma axis. Biomed Pharmacother. 2019;120:109462.

[11] Xin L, Liu L, Liu C, et al. DNA-methylation-mediated silencing of miR-7-5p promotes gastric cancer stem cell invasion via increasing Smo and Hes1. J Cell Physiol. 2020;235(3):2643–2654.

[12] Ye T, Yang M, Huang D, et al. MicroRNA-7 as a potential therapeutic target for aberrant NF-kappaB-driven distant metastasis of gastric cancer. J Exp Clin Cancer Res. 2019;38(1):55.

[13] Yang Z, Shi X, Li C, et al. Long non-coding RNA UCA1 upregulation promotes the migration of hypoxia-resistant gastric cancer cells through the miR-7-5p/EGFR axis. Exp Cell Res. 2018;368(2):194–201.

[14] Liu Z, Jiang Z, Huang J, et al. miR-7 inhibits glioblastoma growth by simultaneously interfering with the PI3K/ATK and Raf/MEK/ERK pathways. Int J Oncol. 2014;44(5):1571–1580.

[15] Hsiao YC, Yeh M-H, Chen Y-J, et al. Lapatinib increases motility of triple-negative breast cancer cells by decreasing miRNA-7 and inducing Raf-1/MAPK-dependent interleukin-6. Oncotarget. 2015;6(35):37965–37978.

[16] Hsieh YH, Jeng SY, et al. Ginsenoside Rh2 ameliorates lipopolysaccharide-induced acute lung injury by regulating the TLR4/PI3K/Akt/mTOR, Raf-1/MEK/ERK, and Keap1/Nrf2/HO-1 signaling pathways in mice. Nutrients. 2018;10:9.

[17] Meng F, Ding J, Liu N, et al. Inhibition of gastric cancer angiogenesis by vector-based RNA interference for Raf-1. Cancer Biol Ther. 2005;4(1):113–117.

[18] Sugimura K, Miyata H, Tanaka K, et al. Let-7 expression is a significant determinant of response to chemotherapy through the regulation of IL-6/STAT3 pathway in esophageal squamous cell carcinoma. Clin Cancer Res. 2012;18(18):5144–5153.

[19] Xu CL, Cheng H, Li N, et al. Relationship between microRNA-27a and efficacy of neoadjuvant chemotherapy in gastric cancer and its mechanism in gastric cancer cell growth and metastasis. Biosci Rep. 2019;39:5.

[20] Pan H, Li T, Jiang Y, et al. Overexpression of circular RNA ciRS-7 abrogates the tumor suppressive effect of miR-7 on gastric cancer via PTEN/PI3K/AKT signaling pathway. J Cell Biochem. 2018;119(1):440–446. .

[21] Zhao X, Dou W, He L, et al. MicroRNA-7 functions as an anti-metastatic microRNA in gastric cancer by targeting insulin-like growth factor-1 receptor. Oncogene. 2013;32(11):1363–1372. .

[22] Sterea AM, Egom EE, El Hiani Y. TRP channels in gastric cancer: new hopes and clinical perspectives. Cell Calcium. 2019;82:102053.

[23] Kong D, Piao Y-S, Yamashita S, et al. Inflammation-induced repression of tumor suppressor miR-7 in gastric tumor cells. Oncogene. 2012;31(35):3949–3960.

[24] Meng F, Dong B, Li H, et al. RNAi-mediated inhibition of Raf-1 leads to decreased angiogenesis and tumor growth in gastric cancer. Cancer Biol Ther. 2009;8(2):174–179.
[25] Liang MI, Prendergast EN, Staples JN, et al. Prognostic role of pathologic response and cytoreductive status at interval debulking surgery after neoadjuvant chemotherapy for advanced epithelial ovarian cancer. J Surg Oncol. 2019. DOI:10.1002/jso.25612.
[26] Tan B, Li Y, Di Y, et al. Clinical value of peripheral blood microRNA detection in evaluation of SOX regimen as neoadjuvant chemotherapy for gastric cancer. J Clin Lab Anal. 2018;32(4):e22363.
[27] Xu N, Lian YJ, Dai X, et al. miR-7 increases cisplatin sensitivity of gastric cancer cells through suppressing mTOR. Technol Cancer Res Treat. 2017;16:1022–1030.
[28] Xie J, Chen M, Zhou J, et al. mir-7 inhibits the invasion and metastasis of gastric cancer cells by suppressing epidermal growth factor receptor expression. Oncol Rep. 2014;31(4):1715–1722.
[29] Chen W, Yu Y, Yang N, et al. Effects of Yangzheng Sanjie decoction-containing serum mediated by microRNA-7 on cell proliferation and apoptosis in gastric cancer. Oncol Lett. 2018;15(3):3621–3629.